Electronic Interactions between π-Stacked Chromophores in Nonsymmetric Tertiary Naphthyl Di- and Polyarylureas

Grace B. Delos Santos and Frederick D. Lewis*

Department of Chemistry, Northwestern University, Evanston, Illinois 60208-3113

Received: May 9, 2005

The synthesis, structure, and spectroscopy of a family of tertiary di- and polyarylureas possessing a naphthyl and several different arene end groups separated by a variable number of internal phenylenediamine linking groups are reported. Molecular modeling and ^{1}H NMR chemical shift data are consistent with the formation of compact, folded structures in which the arene groups adopt a splayed face-to-face geometry. The structure and solvent dependence of the electronic absorption and emission spectra have been determined and are interpreted with the aid of ZINDO calculations. The electronic absorption spectra are relatively insensitive to the choice of arene end group, the number of linking groups, and the solvent polarity. In contrast, the solution fluorescence is highly dependent upon the structure and solvent polarity. These observations are attributed to a small change in polarity upon excitation of the ground state to a naphthalene-localized Franck−Condon singlet state, which can undergo relaxation to a highly polar emissive state with extensive charge-transfer character.

Introduction

Electronic interactions between the π-stacked aromatic rings of chromophore arrays are of interest in studies of both natural and synthetic systems. Examples of natural systems include the light harvesting antennae of green plants and photosynthetic bacteria[1] and the π-stacked base pairs of duplex DNA.[2] Examples of synthetic systems include self-aggregating chromophores such as perylenediimide,[3] oligomers such as oligofluorenes,[4,5] aromatic foldamers,[6] and tertiary oligophenylureas,[7,8] and multilayered cyclophanes.[9] Most of these examples involve either repetitive use of a single chromophore or alternating donor and acceptor chromophores. Exceptions include some multilayer cyclophanes[10] and DNA conjugates with donor and acceptor groups at either end.[11]

We have investigated ground- and excited-state electronic interactions in a number of symmetrical tertiary diarylureas and oligomeric phenyl ureas containing one to four urea linkers.[8,12−14] These molecules adopt compact folded structures in which the arenes are loosely π-stacked, in preference to extended unfolded structures. Excitonic interactions between the π-stacked chromophores result in blue-shifted absorption and fluorescence spectra. We recently reported the synthesis of several nonsymmetric tertiary arylureas possessing naphthalene and nitrobenzene end groups in which excitation of the naphthalene chromophore results in efficient energy transfer to nitrobenzene.[15] Our search for urea-based π-stacked donor−bridge−acceptor (DBA) systems that might undergo efficient long-range electron transfer led us to investigate nonsymmetric tertiary ureas with naphthyl and arene end groups separated by zero, one, or two internal phenylenediamines (Chart 1). The room-temperature fluorescence of these systems is strongly dependent upon the choice of end group, the number of arene rings, and the solvent polarity. The formation of highly polar CT singlet states is observed when the end group is an electron donor but not when it is an electron acceptor.

CHART 1

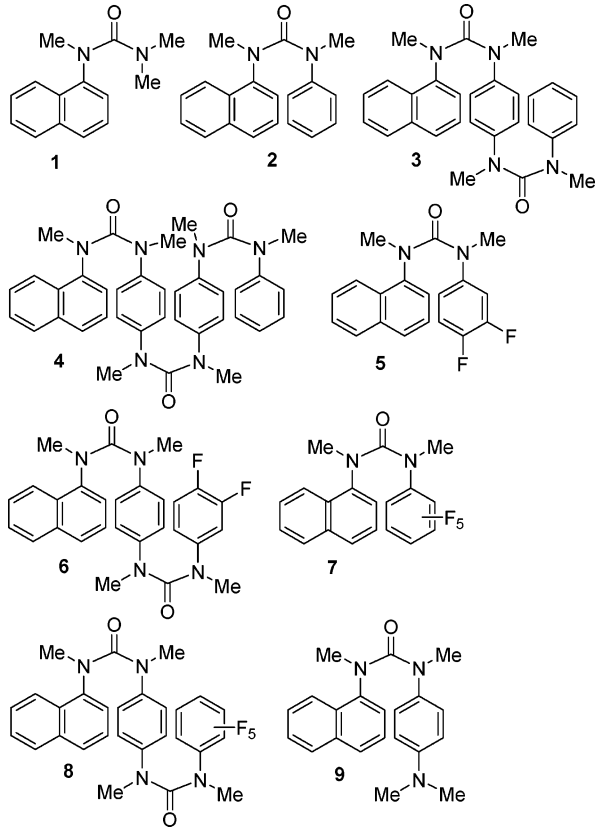

Experimental Section

General. ^{1}H NMR spectra for methylated compounds were measured at 400 or 500 MHz in $CDCl_3$ solution with TMS as

* To whom correspondence should be addressed. E-mail: lewis@chem.northwestern.edu.

10.1021/jp052406+ CCC: $30.25
Published on Web 08/18/2005

internal standard. Chemical shifts (δ) are quoted in parts per million. J values are given in hertz. UV−vis spectra were measured on a Perkin-Elmer Lambda 2 UV−vis spectrometer using a 1 cm path length quartz cell. Total emission spectra were measured on a SPEX Fluoromax spectrometer. Low-temperature spectra were measured in a Suprasil quartz EPR tube (i.d. = 3.3 mm) using a quartz liquid nitrogen coldfinger Dewar at 77 K. Total emission quantum yields were measured by comparing the integrated area under the total emission curve at an equal absorbency and the same excitation wavelength as those of an external standard, 9,10-diphenyl anthracene ($\Phi_f \approx 0.9$ at 298 K).[16] Emission spectra are uncorrected, and the estimated error for the quantum yields is ±10%. Fluorescence decays were measured on a PTI Timemaster fluorescence time-based detection instrument excited with a gated nitrogen-filled lamp as the excitation source. Nonlinear least-squares fitting of the decay curves employed the Levenburg−Marquardt algorithm as described by James et al.[17] and implemented by the Photon Technologies International Timemaster (version 1.2) software. Goodness of fit was determined by judging the χ^2 (<1.2 in all cases), the residuals, and the Durbin−Watson parameter (>1.6 in all cases).

INDO/S-CIS-SCF (ZINDO) calculations (26 occupied and 26 unoccupied frontier orbitals) were performed on a PC with the ZINDO Hamiltonian as implemented by CAChe, release 6.1.10.[18] Calculated absorption spectra for **2**−**9** are provided as Supporting Information. All molecular models used in the semiempirical calculations were based on AM1 optimized ground-state geometries by using the MOPAC suite of programs as implemented under CAChe, release 6.1.10.[18] All data-fitting procedures were carried out by using Origin (version 6.1).[19]

Materials. The syntheses of 1,1,3-trimethyl-3-naphthalen-1-ylurea (**1**) and 1,3-dimethyl-1-naphthalen-1-yl-3-phenylurea (**2**) have been previously described.[15] Procedures for the preparation of ureas **3**−**9** are provided in Supporting Information.

1-[4-(1,3-Dimethyl-3-naphthalen-1-ylureido)phenyl]-1,3-dimethyl-3-phenylurea (3). ^{1}H NMR ($CDCl_3$, 500 MHz): δ 2.75 (s, 3H), 3.04 (m, 6H), 3.24 (s, 3H), 6.11 (d, J = 8.5, 2H), 6.18 (d, J = 8.5, 2H), 6.61 (d, J = 8.0, 2H), 6.84 (dd, J = 7.5, J = 7.5, 1H), 6.93 (m, 3H), 7.15 (dd, J = 7.5, J = 7.5, 1H), 7.31 (m, 2H), 7.48 (d, J = 8.0, 1H), 7.54 (d, J = 7.5, 1H), 7.63 (d, J = 8.0, 1H). MS calcd for $C_{28}H_{28}N_4O_2$ m/z 452.5; found, 452.2.

Urea (4). ^{1}H NMR ($CDCl_3$, 500 MHz): δ 2.69 (s, 3H), 2.92 (s, 3H), 2.99 (m, 6H), 3.11 (s, 3H), 3.23 (s, 3H), 6.09 (d, J = 9.0, 2H), 6.18 (d, J = 8.5, 2H), 6.31 (d, J = 8.5, 2H), 6.38 (d, J = 8.5, 2H), 6.70 (d, J = 7.5, 2H), 6.89 (m, 1H), 6.93 (d, J = 7.5, 1H), 7.15 (m, 2H), 7.15 (m, 1H), 7.31 (m, 2H), 7.48 (d, J = 8.0, 1H), 7.53 (d, J = 7.0, 1H), 7.62 (d, J = 7.0, 1H). MS calcd for $C_{37}H_{38}N_6O_3$ m/z 614.7; found, 614.3.

1-(3,4-Difluorophenyl)-1,3-dimethyl-3-naphthalen-1-ylurea (5). ^{1}H NMR ($CDCl_3$, 500 MHz): δ 3.09 (s, 3H), 3.32 (s, 3H), 6.21 (d, J = 9.0, 1H), 6.29 (ddd, J = 2.0, J = 7.5, J = 10.0, 1H), 6.49 (dd, J = 18.5, J = 9.0, 1H), 6.96 (d, J = 7.5, 1H), 7.22 (dd, J = 7.5, J = 7.5, 1H), 7.42 (m, 2H), 7.60 (d, J = 8.5, 1H), 7.63 (dd, J = 6.0, J = 1.8, 1H), 7.74 (dd, J = 6.3, J = 3.5, 1H). MS calcd for $C_{19}H_{16}F_2N_2O$ m/z 326.3; found, 326.2.

1-(4-[3-(3,4-Difluorophenyl)-1,3-dimethylureido]phenyl)-1,3-dimethyl-3-naphthalen-1-ylurea (6). ^{1}H NMR ($CDCl_3$, 500 MHz): δ 2.57 (s, 3H), 2.99 (s, 3H), 3.06 (s, 3H), 3.25 (s, 3H), 6.11 (d, J = 8.5, 2H), 6.27 (d, J = 8.5, 2H), 6.36 (m, 2H), 6.73 (dd, J = 10, J = 20, 1H), 6.97 (d, J = 7.5, 1H), 7.16 (dd, J = 7.5, J = 7.5, 1H), 7.32 (m, 2H), 7.49 (d, J = 8.5, 1H), 7.55 (d, J = 9.0, 1H), 7.63 (d, J = 7.5, 1H). MS calcd for $C_{28}H_{26}F_2N_4O_2$ m/z 488.5; found, 488.2.

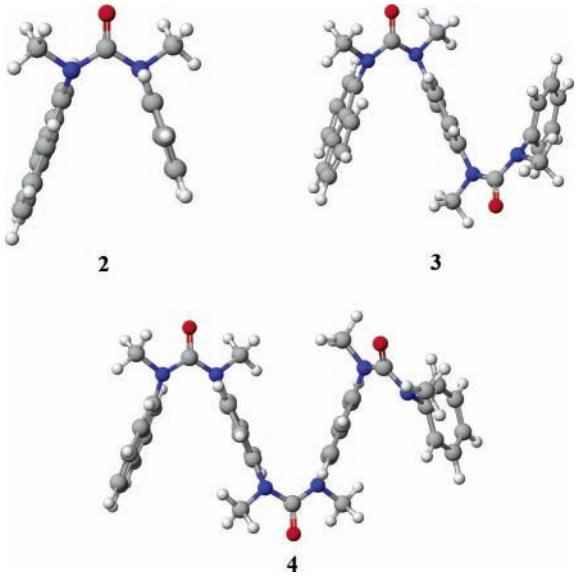

Figure 1. AM1 minimized structures for naphthylarylureas **2**−**4**.

1,3-Dimethyl-1-naphthalen-1-yl-3-pentafluorophenylurea (7). ^{1}H NMR ($CDCl_3$, 500 MHz): δ 3.12 (s, 3H), 3.33 (s, 3H), 7.19 (d, J = 8.5, 1H), 7.33 (dd, J = 8.5, J = 8.5, 1H), 7.45 (d, J = 8.5, 1H), 7.48 (d, J = 8.5, 1H), 7.64 (d, J = 8.5, 1H), 7.69 (d, J = 8.5, 1H), 7.75 (d, J = 8.5, 1H). MS calcd for $C_{19}H_{13}F_5N_2O$ m/z 380.3; found, 380.2.

1-[4-(1,3-Dimethyl-3-pentafluorophenylureido)phenyl]-1,3-dimethyl-3-naphthalen-1-ylurea (8). ^{1}H NMR ($CDCl_3$, 500 MHz): δ 2.79 (s, 3H), 2.99 (s, 3H), 3.06 (s, 3H), 3.26 (s, 3H), 6.20 (d, J = 8.5, 2H), 6.33 (d, J = 8.5, 2H), 6.98 (d, J = 7.0, 1H), 7.17 (dd, J = 7.5, J = 7.5, 1H), 7.32 (m, 2H), 7.49 (d, J = 8.0, 1H), 7.54 (d, J = 7.5, 1H), 7.63 (d, J = 7.0, 1H). MS calcd for $C_{28}H_{23}F_5N_4O_2$ m/z 542.5; found, 542.2.

1-(4-Dimethylaminophenyl)-1,3-dimethyl-3-naphthalen-1-yl-urea (9). ^{1}H NMR ($CDCl_3$, 400 MHz): δ 2.65 (s, 6H), 3.09 (s, 3H), 3.27 (s, 3H), 6.07 (d, J = 8.4, 2H), 6.31 (d, J = 8.4, 2H), 6.93 (d, J = 7.2, 1H), 7.20 (m, 1H), 7.35 (m, 2H), 7.52 (m, 1H), 7.67 (m, 2H). MS calcd for $C_{21}H_{23}N_3O$ m/z 333.4; found, 333.2.

Results and Discussion

Molecular Structure. The synthesis of the naphthylureas **1** and **2** has previously been described.[15] Detailed procedures employed for the synthesis of ureas **3**−**9** are provided as Supporting Information. ^{1}H NMR and mass spectral data (see Experimental Section) are consistent with the assigned structures.

Gas-phase structures for ureas **2**−**4** obtained from AM1 calculations are shown in Figure 1.[18] The completely folded conformations are more stable than are conformations in which the naphthyl ring is in an extended conformation by ~2 kcal/mol. The preference of tertiary di- and polyarylureas for folded vs extended conformations has previously been observed for polyphenylureas and polynaphthylureas.[7] This preference is steric in origin, nonbonded methyl−methyl or methyl-aryl repulsion in the extended conformations being larger than the face-to-face aryl−aryl interactions in folded conformations. The preference for folded vs extended conformations is larger for the pentafluorophenyl **7** vs phenylurea **2**, and the naphthyl−phenyl plane-to-plane distances are slightly shorter for **7**. These

TABLE 1: ^{1}H NMR Chemical Shifts for Selected Protons[a] and Calculated Dipole Moments[b]

	δ (ppm)			
urea	naphthyl H_2	inner phenyl	outer phenyl	μ (D)
1	7.19			
2	6.88		6.51, 6.66, 6.76	3.10
3	6.93	6.11, 6.18	6.61, 6.93, 6.84	2.61
4	6.93	6.09, 6.18 (6.31, 6.38)[c]	6.70, 6.98, 6.89	3.72
5	6.96		6.21, 6.29, 6.49	1.92
6	6.97	6.11, 6.27	6.34, 6.73, 6.38	4.28
7	7.19		*d*	2.08
8	6.98	6.20, 6.33	*d*	2.48
9	6.93		6.07, 6.31	4.09

[a] Chemical shifts in CD_3Cl solution. [b] Calculated dipole moment obtained from ZINDO calculations. [c] Inner phenyl distal from naphthalene. [d] Pentafluorophenyl systems.

differences may reflect decreased π-electron repulsion for the pentafluorophenyl as a consequence of its inverted electronic structure, e.g., electron-rich perimeter and electron-poor face.[20]

The ^{1}H NMR spectra of **2**−**9** in CD_3Cl are consistent with folded structures in solution. Chemical shifts for the H_2 protons of the naphthalene and the protons of the phenyl rings are summarized in Table 1. The naphthyl H_2 protons are shifted downfield in the series **7** > **5** > **2**, in order of the electron-withdrawing abilities of the phenyl, difluorophenyl, and pentafluorophenyl groups. The intervening phenyl groups in **6** and **8** insulate the naphthyl group from this shielding effect. Upfield shifts are also observed for the inner phenyl rings in ureas **3**, **4**, **6**, and **8**. The protons of the inner rings are nonequivalent, the ortho protons nearest the point of attachment to naphthylurea linker occurring upfield of the other protons. The protons on the second inner phenyl ring of **4** are less shielded than are those of the first inner phenyl ring, reflecting the greater shielding effect of naphthyl vs phenyl rings. Shielding of the outer phenyl rings also decreases as the distance from naphthyl increases in ureas **2**−**4**. The chemical shifts for **3** are similar in CD_3Cl and CD_3CN solutions, indicating that the preference for folded structures is independent of solvent polarity.

Ground-state dipole moments (Table 1) were calculated using the semiempirical Hartree−Fock intermediate neglect of differential overlap method (INDO) as parametrized by Zerner and co-workers (ZINDO) and implemented in CAChe 6.1.10.[18] The results are consistent with alignment of the dipoles with the carbonyl C═O axis, as is the case for other diarylurea derivatives.[21] The calculated dipoles for the diarylureas increase as the phenyl substituent becomes more donating, **7** ∼ **5** < **2** < **9**. The dipole moment of the triarylurea **3** is smaller than that of either the diarylurea **2** or the tetraarylurea **4**, in accord with molecular dipoles that are determined by the vector sum of the carbonyl dipoles in folded conformations (Figure 1).

Electronic Absorption Spectra. The electronic absorption spectra of ureas **1**−**9** in methylcyclohexane solution are shown in Figure 2. A well-resolved long wavelength band at ∼290 nm is observed for the diarylureas **2**, **5**, **7**, and **9**. In the case of **9** a second maximum is observed at 265 nm. The 290 nm band appears as a shoulder on the stronger 260 nm bands of the tri- and tetraarylureas **3**, **4**, **6**, and **8**. The spectra of the tetraarylureas can be fit well by the sum of two Gaussians with maxima at 298 and 253 nm. The spectra of di- and triarylureas with phenyl, difluorophenyl, and pentafluorophenyl end groups are similar in band shape. Absorption maxima for **1**−**9** in the solvents methylcyclohexane (MCH), 2-methyltetrahydrofuran (MTHF), and acetonitrile (MeCN) are summarized in Table 2. Only small solvent-induced shifts in the absorption maxima are observed,

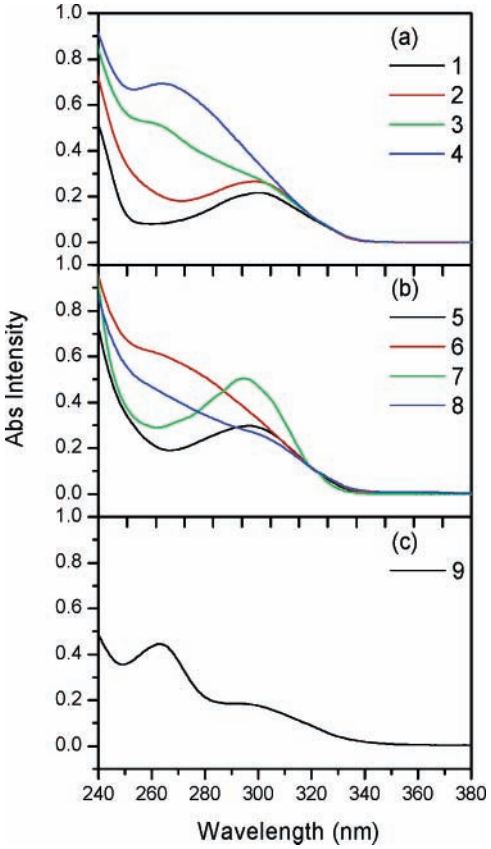

Figure 2. UV−vis absorption spectra in MCH for ureas **1**−**9**.

indicative of similar polarities for the ground state and Franck−Condon singlet state.

The electronic structure and absorption spectra of ureas **2**−**8** were investigated using ZINDO calculations.[22] Selected frontier orbitals for ureas **2**, **7**, and **9** are shown in Figure 3. The calculated wavelength, molar absorbance, and character of the lowest singlet states for these diarylureas and the triarylurea **3** are reported in Table 3. A complete set of frontier orbitals and a table summarizing the calculated properties of the singlet states for **2**−**9** is provided in Supporting Information.

The HOMO and LUMO orbitals of urea **2** are naphthalene-localized, as are the HOMO of **7** and the LUMO of **9**. However, the LUMO of **7** is phenyl-localized and the HOMO of **9** is delocalized. In all cases the lowest energy allowed transition is dominated by the HOMO−LUMO transition (corresponding to naphthalene ^1L_a),[16] with varying extents of configuration interaction (CI) but similar energies (284−290 nm). Several weakly allowed transitions lie at lower energies. In most cases, the lowest energy transitions have similar calculated energies (318−319 nm) and are naphthalene-localized with more extensive CI (corresponding to naphthalene ^1L_b). At slightly higher energies are found transitions that can be described as n → π^* (urea-localized to delocalized) with extensive CI involving HO−5 and similar filled orbitals and LU+4 and similar vacant orbitals (Figure 3). In the case of **7** the lowest energy transition is described by ZINDO as having delocalized n,σ^* character (urea−fluorobenzene delocalized to urea−fluorobenzene σ-antibonding). The 260 nm band present in the spectrum of **9** and in the deconvoluted spectra of **3**, **4**, **6**, and **8** are assigned to π,π^* transitions localized on the phenyl rings. They have energy and intensity similar to the corresponding transitions of the analogous polyphenylureas.[8]

ZINDO calculations were also carried out on the extended conformer of **3**. The naphthalene-like ^1L_a and ^1L_b transitions

TABLE 2: Absorption and Fluorescence Data for the Naphthylarylureas

urea	solvent[a]	λ_{abs} (nm)	λ_{fl} (nm)[c]	Φ_f [c]	τ_S (ns)[c]	k_f (10^7 s^{-1})[d]
1	MCH	296	359	0.03	1.1	2.7
	MTHF	296	367	0.09	1.2	7.5
	MeCN	294	374	0.016	0.67	2.4
2	MCH	293	358	0.011	1.9	0.58
	MTHF	294	406	0.012	3.0	0.40
	MeCN	294	441	0.015	6.4	0.23
3	MCH	298	421	0.011	2.3	0.48
	MTHF	262 (297[b])	485	0.010	5.8	0.17
	MeCN	299[b]	355	0.052	0.6	
4	MCH	262	424	0.009	3.1	0.29
	MTHF	263	395	0.004	4.3	
			484	0.007	6.3	0.32
	MeCN	263	388	0.002		
			524			
5	MCH	292	358	0.18	0.80	22.5
	MTHF	290	364	0.024	5.6	0.43
	MeCN	292	376			
6	MCH	297[b]	416	0.017	1.6	1.0
	MTHF	297[b]	477	0.011	6.5	0.17
	MeCN	296[b]	527			
7	MCH	290	354	0.02	2.7	0.74
	MTHF	290	372	0.002	3.0	
	MeCN	289	372		3.6	
8	MCH	292	372	0.004		
	MTHF	298[b]	452	0.005	1.6	0.31
	MeCN	300[b]	355			
9	MCH	263 (299)[b]	358	0.01	2.5	
			458	0.02	5.4	0.37
	MTHF	265 (299)[b]	361			
			543			
	MeCN	265 (300)[b]	361			

[a] MCH = methylcyclohexane, MTHF = 2-methyltetrahydrofuran, MeCN = acetonitrile. [b] Absorption maxima obtained from the absorption spectrum of the sum of two Gaussian bands; $R^2 > 0.999$. [c] Fluorescence emission maxima, quantum yields, and decay times determined for deoxygenated solutions at room temperature. [d] Fluorescence decay time $k_f = \Phi_f(\tau_s^{-1})$.

are more localized than is the case for the folded transitions. Other more delocalized frontier orbitals are confined to the diphenylurea portion of the molecule. Thus, the extended conformer is expected to display absorption and emission spectra characteristic of the parent naphthalene ^1L_b state.

Room-Temperature Fluorescence Spectra. The fluorescence spectra of ureas **2**−**9** in MCH, MTH, and MeCN solution at room temperature are shown in Figure 4, and fluorescence maxima are summarized in Table 2. The fluorescence spectra of **1** and **2** have been reported previously.[14,15] Dual fluorescence is observed in some solvents for **9** and for the tri- and tetraarylureas, consisting of a short wavelength band having a maximum that is weakly dependent upon solvent polarity and a long wavelength band that is strongly solvent-dependent. Plots of the solvent-dependent emission maxima vs the Lippert−Mataga solvent polarity parameter Δf,

$$\Delta f = \frac{\epsilon - 1}{2\epsilon + 1} - \frac{n^2 - 1}{4n^2 + 2} \quad (1)$$

are shown in Figure 5.[23]

The appearance of the fluorescence spectra (Figure 4) is dependent upon the nature of the aryl substituents, the number of aryl rings, and the solvent polarity. The spectra of ureas **1**, **2**, **5**, and **7** in MCH are broadened and red-shifted when compared to the fluorescence of naphthalene (λ_{fl} = 322 nm). Weak vibronic structure is observed in MCH solution only for the fluorescence of **5**. The fluorescence spectrum of **9** in MCH is dominated by a long wavelength band, which is significantly red-shifted when compared to the spectra of the other diarylureas (the shorter wavelength band will be discussed later). The emission spectra of the tri- and tetraarylureas **3**, **4**, **6**, and **8** in MCH solution have maxima between those of **9** and the other diarylureas. The long wavelength emission maxima in the

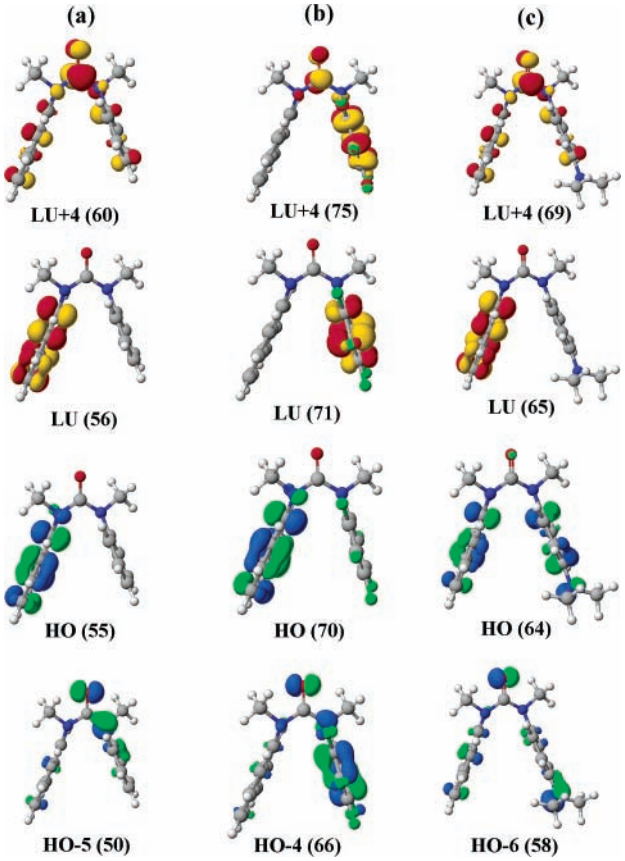

Figure 3. Selected ZINDO molecular orbitals for (a) **2**, (b) **7**, and (c) **9**.

TABLE 3: Calculated Properties of Selected Singlet States[a]

urea	state	λ (nm)	A	character[b]
2	S_1	319	1033	Np π,π^* ^1L_b
	S_2	316	337	urea n,π^* CI
	S_3	290	16230	Np π,π^* ^1L_a
3	S_1	318	964	Np π,π^* ^1L_b
	S_2	314	372	urea n,π^* CI
	S_3	313	248	urea n,π^* CI
	S_4	293	1138	inner Ph CI
	S_5	288	17283	Np π,π^* ^1L_a
7	S_1	319	1019	π,σ^* CI
	S_2	313	478	Np π,π^* ^1L_b
	S_3	301	758	F_5 π,π^* CI
	S_4	293	612	Np-F_5 π,π^* CI
	S_5	289	12303	Np π,π^* ^1L_a
9	S_1	319	1001	Np-DMA $\pi-\pi^*$ CI
	S_2	315	306	urea n,π^* CI
	S_3	297	1966	aniline π,π^*
	S_4	290	15030	Np π,π^* ^1L_a

[a] Singlet state energies, molar absorbance, and character based on ZINDO calculations. See Figure 3. [b] Np π,π^* ^1L_b is a naphthalene-localized state with CI between two π,π^* transitions. Urea n,π^* is dominated by several transitions from delocalized urea nonbonding orbitals to delocalized π orbitals (e.g., HO−5 to LU+4 for **2**) with extensive CI. Np π,π^* ^1L_a is the HO−LU transition. π,σ^* CI is dominated by several transitions from bonding to antibonding urea−fluorophenyl (e.g., HO−4 to LU+4 for **7**). Np-DMA is dominated by several transitions involving delocalized π bonding and antibonding orbitals.

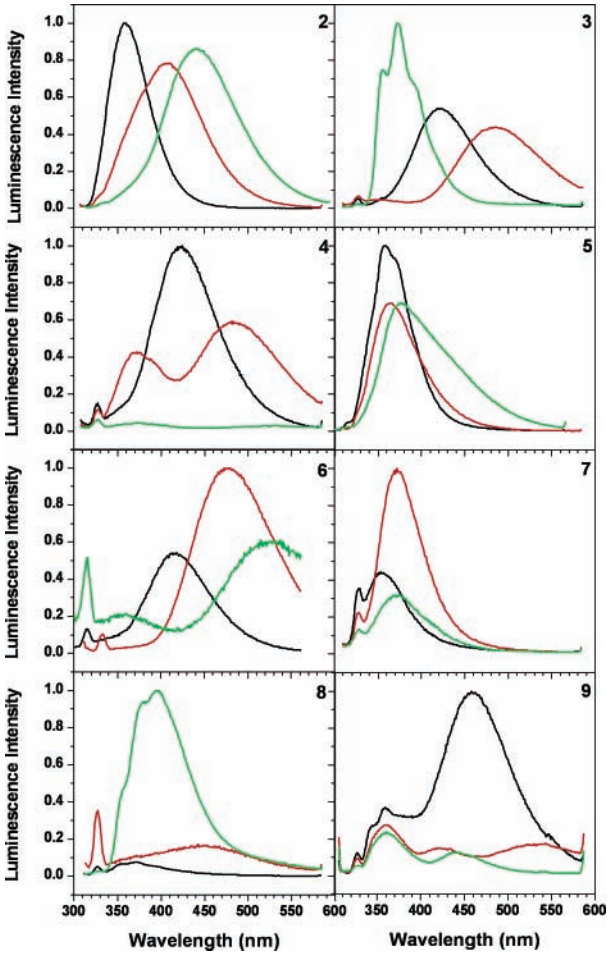

Figure 4. Room-temperature fluorescence spectra for **2**−**9** in MCH (black), MTHF (red), and MeCN (green).

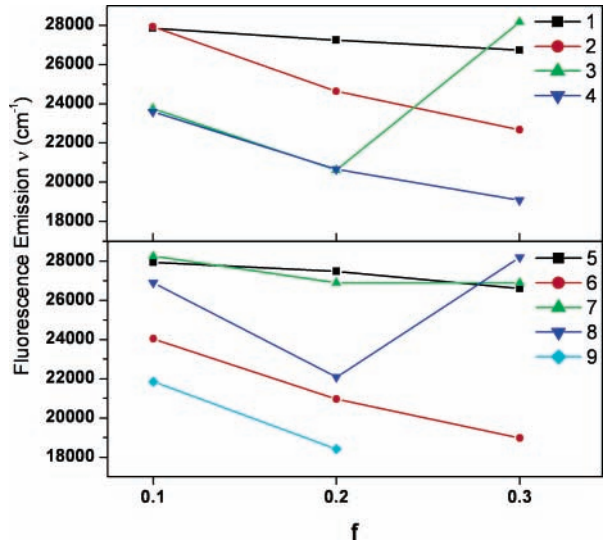

Figure 5. Solvatochromic plot of fluorescence emission frequency for **1**−**9**.

moderately polar solvent MTHF are red-shifted with respect to those in MCH, the magnitude of the solvent-induced shifts being smaller for **1**, **5**, and **7** than for the other ureas (Figure 5). Further red-shifts are observed in MeCN solution for some of the ureas but not for **3**, **8**, and **9**.

The large solvent-induced fluorescence shift observed for urea **9** in MTHF is indicative of a fluorescent singlet state having extensive charge-transfer (CT) character,[24] in which naphthalene

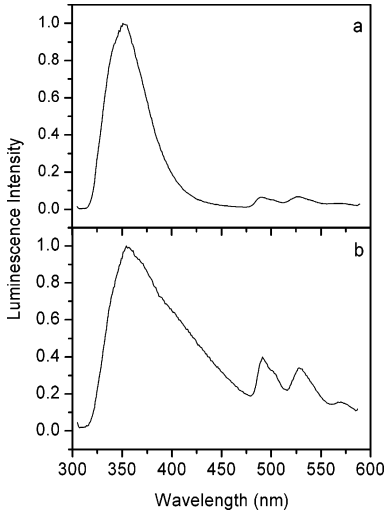

Figure 6. Emission spectra at 77 K in MTHF for (a) **2** and (b) **3**.

serves as an electron acceptor and dimethylaniline serves in its usual role as an electron donor. The smaller solvent-induced shifts observed for the tri- and tetraarylureas **3**, **4**, **6**, and **8** are consistent with the central phenylenediamine serving as a weaker electron donor than dimethylaniline. The electron-withdrawing effect of the urea carbonyl groups on both of the phenylenediamine nitrogens should render it a weaker donor than the dimethylaniline end group of **9**. The fluorinated diarylureas **5** and **7** display very small solvent-induced shifts, similar to those for **1**, in accord with the inability of the fluorinated benzene derivatives to serve as electron donors. In summary, both the emission maxima in the nonpolar solvent MCH and the solvent-induced shifts in the more polar solvents MTHF and MeCN are consistent with emission from singlet states with varying degrees of CT character, determined by the electron-donating ability of the arene ring adjacent to naphthalene which follows the order aniline > phenylenediamine > phenyl > fluorophenyl. In the case of the tri- and tetraarylureas, the maxima in MCH and the solvent-induced shifts are similar for **3**, **4**, and **6**. The shorter wavelength for the maximum of **8** in MCH can be attributed to the stronger inductive electron-withdrawing effect of the pentafluorophenyl group.[20]

The fluorescence spectrum of **9** in MCH solution and the spectra of several of the other diarylureas in MTHF or MeCN display short wavelength bands with maxima similar to that of **1**. In the case of **4** in MTHF and **9** in MeCN, the ratio of these bands is dependent upon the excitation wavelength, excitation in the red-edge of the absorption band (280−300 nm) favoring the short wavelength emission and excitation near the absorption maximum (260 nm) favoring the long wavelength emission. The excitation wavelength dependence of the ratio of short vs long wavelength bands is indicative of the presence of two emissive ground-state species. Similar dual fluorescence has been observed for tertiary dipyrenylureas in MTHF and was attributed to low populations of extended conformations of the diarylureas.[13]

Low-Temperature Emission Spectra. The total luminescence spectra of ureas **2** and **3** in MTHF glasses at 77 K are shown in Figure 6. The weak structured long wavelength emission observed for all of the arylureas is attributed to naphthalene-localized phosphorescence. The shorter wavelength emission of **2** (Figure 6a) is attributed to naphthalene-localized fluorescence. Similar short wavelength spectra are observed for **1**, **5**, **7**, and **8**. The effect of temperature on the fluorescence spectra of **2** is similar to that previously observed for the

SCHEME 1

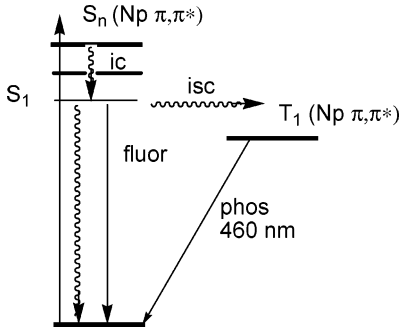

analogous tertiary dinaphthylurea.[14] Evidently the red-shifted emission observed in fluid solution requires a large-amplitude change in the geometry of the locally excited singlet state prior to fluorescence. The relaxed singlet presumably has a more sandwich-like excimer geometry rather than the splayed-ring geometry of the ground state. The fluorescence spectra of **3** (Figure 6b) and **6** (spectrum not shown) at 77 K are broad and asymmetric when compared to that of **2**. This may reflect stronger electronic coupling of naphthalene with the internal phenylene diamine rings of **3** and **6** vs the phenyl group of **2**.

Fluorescence Quantum Yields and Lifetimes. Quantum yields for room-temperature fluorescence and fluorescence decay times for ureas **1**−**9** are reported in Table 2. The quantum yields and decay times for both components of **4** in MTHF and **9** in MCH are reported. In all other cases data for the major component are reported. The fluorescence quantum yields for the long wavelength fluorescence bands are generally quite small ($\leq$0.02), whereas larger quantum yields are observed for **1** in all solvents and for the short wavelength components of **3** in MeCN and **5** in MCH. The fluorescence decay times are in the range 0.6−6.5 ns and display no consistent pattern that can be correlated with urea structure or solvent polarity.

Fluorescence rate constants can be calculated from the quantum yields and lifetime data for the long wavelength fluorescence components if it is assumed that this emission occurs from folded conformational isomers that absorb most of the 300 nm excitation used for the quantum yield measurements. The calculated values of k_f for **2**−**9** (excepting the value for **5** in MCH) lie in the range $(0.2-1.0) \times 10^7$ s^{-1}. Again, no consistent correlation with structure or solvent polarity is observed. These values are somewhat shorter than the value for **1** or for the tertiary dinaphthylureas.[14] These differences may reflect a change in the character of the emissive singlet state, as discussed below.

The fluorescence and phosphorescence quantum yields for **2** at 77 K in MTHF are 0.31 and 0.02, respectively, and the phosphorescence decay time is 1.4 s.[15] The low phosphorescence quantum yield and long decay time are similar to those of unsubstituted naphthalene.[25]

Formation and Decay of the Fluorescent Singlet State. The photophysical behavior of the folded tertiary naphthylarylylureas can be summarized in the state energy diagram shown in Scheme 1. The lowest energy allowed transitions of **2**−**9** are identified by the ZINDO calculations as a naphthalene-localized π,π^* transitions, dominated by the HO−LU one-electron configuration, similar in character to the naphthalene ^1L_a transition. Excitation near the 300 nm maxima or shoulders in the absorption spectra (Figure 2) most likely populates this upper singlet state S_n ($n = 3-7$, depending upon the number of aryl groups in **2**−**9**).

The identity of the fluorescent states is less certain and most likely depends on the choice of aryl group and solvent polarity. The gas-phase ZINDO calculations indicate the presence of a weaker naphthalene-localized low-energy transition with extensive CI for **2**−**9**. These transitions are similar in character to the naphthalene ^1L_b transition. The small solvent-induced shifts for **1**, **5**, and **7** in fluid solution (Figure 5) is consistent with fluorescence from a ^1L_b state in solution and for all of the ureas in low-temperature glasses. The short wavelength fluorescence bands of **3**, **4**, **8**, and **9** can be attributed to the ^1L_b state of the extended (minor) conformers.

A naphthalene-localized state cannot, however, account for the pronounced solvent-induced shifts observed for the other arylureas. Low-energy singlet states such as S_1 for **9** and S_2 for **3**, **4**, and **6** (see Supporting Information) appear to be likely candidates for the fluorescent singlet state (Table 3). On the basis of ZINDO calculations, these states are expected to have significant naphthalene−arene CT character, in accord with their large solvent-induced shifts. Their low calculated oscillator strengths are consistent with the relatively small values of k_f calculated from the fluorescence quantum yields and decay times (Table 2).

The low fluorescence quantum yields for the naphthylarylureas require the presence of a relatively efficient nonradiative decay pathway for the fluorescent singlet state. The low quantum yields for phosphorescence at 77 K suggest that intersystem crossing is not a significant decay pathway. The decrease in fluorescence intensity observed in MeCN solution may reflect more rapid decay of singlet CT states via charge recombination in polar solvent.[26] We have previously reported that tertiary dinaphthylureas undergo intramolecular naphthalene [2 + 2] photodimerization.[14] Nonsynchronous C_1-C_1 bonding was suggested to yield biradical intermediates that could either proceed to products or revert to starting materials. The photochemical behavior of the naphthylarylureas has not been investigated. However, naphthyl−aryl bonding might provide an efficient singlet state nonradiative decay pathway for **2**−**9**.

Concluding Remarks

These results provide the first examples of excited state charge-transfer luminescence from nonsymmetric di- and polyarylureas. The substituent and solvent dependence of the fluorescence maxima is indicative of luminescence from a CT state in which naphthalene serves as an electron acceptor and the arene as an electron donor. We had anticipated that a locally excited naphthylurea singlet state might serve as an electron donor, as is the case for aminonaphthalenes.[27] However, CT fluorescence is observed with dimethylaniline and phenylenediamine donors but not with di- or pentafluorobenzene acceptors. We previously reported that naphthylureas with nitrobenzene acceptors are nonfluorescent as a consequence of the presence of nitrobenzene-localized low-energy dark singlet states.[15] CT luminescence has been observed in preliminary studies of naphthylureas with 4-cyanobenzene or 3,4-dicyanobenzene acceptors.[28]

The luminescence from the tri- and tetraarylureas in this investigation can be assigned to CT states in which naphthalene serves as an electron acceptor and the adjacent bridging phenyl as an electron donor. There is no evidence for more extensive charge delocalization in the excited states of **3** and **4**. It would be interesting to investigate electronic interactions in analogues of **3** and **4** possessing a dimethylaminophenyl donor distal to naphthalene in order to determine if the initially formed CT state would relax to a charge-separated state.

Finally, it is noted that the electronic interactions in tertiary polyarylureas are more complex than those in π-stacked systems

connected by σ-bonded linkers.[4,10] ZINDO calculations indicate that the molecular orbitals and excited states are not rigorously localized on the arene or urea chromophores, even though the arene and urea planes are nearly orthogonal. Thus, the urea linker strongly influences the nature of the electronic interactions in tertiary arylureas. In this respect, the urea linker is similar to the amide linker in tertiary *N*-arylbenzamides.[29]

Acknowledgment. The authors thank Todd Kurth and Weizhong Liu for advice. Funding for this project was provided by NSF Grants CHE-0100596 and CHE-0400663 and by an Undergraduate Research Grant from Northwestern University to G.B.D.S.

Supporting Information Available: Scheme S1 showing the synthetic routes and structures, experimental procedures for the preparation of ureas **3**−**9**, Table S1 listing the properties of the lowest singlet states of ureas **2**−**9**, and Figures S1−S8 showing ZINDO frontier orbitals for ureas **2**−**9**. This material is available free of charge via the Internet at http://pubs.acs.org.

References and Notes

(1) Pullerits, T.; Sundstrom, V. *Acc. Chem. Res.* **1996**, *29*, 381−389.
(2) Lewis, F. D. *Photochem. Photobiol.* **2005**, *81*, 65−72.
(3) Würthner, F. *Chem. Commun.* **2004**, 1564−1579.
(4) Nakano, T.; Yade, T. *J. Am. Chem. Soc.* **2003**, *125*, 15474−15484.
(5) Rathore, R.; Abdelwahed, S. H.; Guzei, I. A. *J. Am. Chem. Soc.* **2003**, *125*, 8712−8713.
(6) Gabriel, G. J.; Iverson, B. L. *J. Am. Chem. Soc.* **2002**, *124*, 15174−15175.
(7) (a) Yamaguchi, K.; Matsumura, G.; Kagechika, H.; Azumaya, I.; Ito, Y.; Itai, A.; Shudo, K. *J. Am. Chem. Soc.* **1991**, *113*, 5474−5475. (b) Krebs, F. C.; Jorgensen, M. *J. Org. Chem.* **2002**, *67*, 7511−7518.
(8) Lewis, F. D.; Kurth, T. L.; Delos Santos, G. *J. Phys. Chem. B* **2005**, *109*, 4893−4899.
(9) Vögtle, F. *Cyclophane Chemistry: Synthesis, Structures, and Reactions*; Wiley: Chichester (U.K.) and New York, 1993.
(10) Machida, H.; Tatemitsu, H.; Otsubo, T.; Sakata, Y.; Misumi, S. *Bull. Chem. Soc. Jpn.* **1980**, *53*, 2943−2952.
(11) Lewis, F. D.; Wu, Y.; Zhang, L.; Zuo, X.; Hayes, R. T.; Wasielewski, M. R. *J. Am. Chem. Soc.* **2004**, *126*, 8206−8215.
(12) (a) Lewis, F. D.; Kurth, T. L.; Liu, W. *Photochem. Photobiol. Sci.* **2002**, *1*, 30−37. (b) Kurth, T. L.; Lewis, F. D.; Hattan, C. M.; Reiter, R. C.; Stevenson, C. D. *J. Am. Chem. Soc.* **2003**, *125*, 1460−1461.
(13) Lewis, F. D.; Kurth, T. L. *Can. J. Chem.* **2003**, *81*, 770−776.
(14) Kurth, T. L.; Lewis, F. D. *J. Am. Chem. Soc.* **2003**, *125*, 13760−13767.
(15) Lewis, F. D.; Delos Santos, G. B.; Liu, W. *J. Org. Chem.* **2005**, *70*, 2974−2979.
(16) Berlman, I. B. *Handbook of Fluorescence Spectra of Aromatic Molecules*, 2nd ed.; Academic Press: New York, 1971.
(17) James, D. R.; Siemiarczuk, A.; Ware, W. R. *Rev. Sci. Instrum.* **1992**, *63*, 1710.
(18) *CAChe*, release 6.1.10; Fujitsu Limited: Miahama-Ku, Chiba City, Chiba, Japan, 2000−2003.
(19) *Origin*, version 6.1; OriginLab Corp.: Northampton, MA, 2000.
(20) (a) Cozzi, F.; Siegel, J. S. *Pure Appl. Chem.* **1995**, *67*, 683−689. (b) Lai, J. S.; Qu, J.; Kool, E. T. *Angew. Chem., Int. Ed.* **2003**, *42*, 5973−5977.
(21) Kutepov, D. F.; Dubov, S. S. *Zh. Obshch. Khim.* **1960**, *30*, 3448−3451.
(22) Zerner, M. C.; Loew, G. H.; Kirchner, R. F.; Mueller-Westerhoff, U. T. *J. Am. Chem. Soc.* **1980**, *102*, 589−599.
(23) (a) Lippert, E. *Z. Electrochem. Angew. Phys. Chem.* **1957**, *61*, 962−975. (b) Mataga, N.; Kaifu, Y.; Koizumi, M. *Bull. Chem. Soc. Jpn.* **1956**, *29*, 465−470.
(24) Grabowski, Z. R.; Rotkiewicz, K.; Rettig, W. *Chem. Rev.* **2003**, *103*, 3899−4032.
(25) Birks, J. B. *Photophysics of Aromatic Molecules*; Wiley-Interscience: London, 1970.
(26) Lewis, F. D.; Weigel, W. *J. Phys. Chem. A* **2000**, *104*, 8146−8153.
(27) Lewis, F. D.; Hougland, J. L.; Markarian, S. A. *J. Phys. Chem. A* **2000**, *104*, 3261−3268.
(28) Kurth, T. L.; Delos Santos, G. B. Unpublished results.
(29) Lewis, F. D.; Liu, W. *J. Phys. Chem. A* **1999**, *103*, 9678−9686.